RSC Advances

ROYAL SOCIETY OF CHEMISTRY

www.rsc.org/advances

Towards understanding the N_{TB} phase: a combined experimental, computational and spectroscopic study

Trpimir Ivšić[a], Marijana Vinković[b], Ute Baumeister[c], Ana Mikleušević[a] and Andreja Lesac[a*]

[a] Division of Organic Chemistry and Biochemistry, Ruđer Bošković Institute, Bijenička cesta 54, 10000 Zagreb, Croatia,

[b] NMR Center, Ruđer Bošković Institute, Bijenička cesta 54, 10000 Zagreb, Croatia,

[c] Institute of Chemistry, Physical Chemistry, Martin Luther University Halle-Wittenberg, von-Danckelmann-Platz 4, 06120 Halle, Germany.

Table of contents entry

Combined experimental, computational and spectroscopic studies support the hierarchical model for the N_{TB} phase that involves formation of embryonic self-assembly of the propeller-shaped dimeric molecules with *syn*-parallel orientation in the isotropic melt.

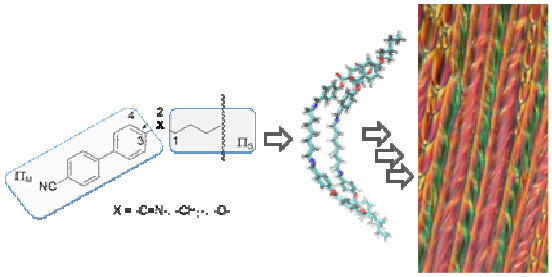

Abstract

Today liquid-crystalline materials are most widely exploited for flat-panel displays, and yet their ability to self-organize into periodically ordered nanostructures gives rise to a broad variety of additional applications. The recently discovered low-temperature nematic phase (N_{TB}) with unusual characteristics generated considerable attention within the scientific community: despite the fact that the molecules from which the phase is composed are not chiral, the helicoidal structure of the phase is strongly implicated. Here we present a combined experimental, computational, and spectroscopic study of the structural aspects influencing the formation of the N_{TB} phase as well as ~~on~~ the possible molecular organization within the phase. In an extensive DFT study, the structure-property prerequisite was traced to a ″bent-propeller″ shape of the molecule. Computational analysis of two possible types of molecular packing suggests that the *syn*-arrangement of dimeric molecules is energetically more favorable than the *anti*-arrangement. The NOESY investigation in the isotropic

melt just prior to the Iso-N transition show the presence of intermolecular interactions that can be attributed to the *syn*-parallel orientation of the mesogens. The synergy of experimental, computational and NMR studies provide a new insight into possible molecular organization within the N_{TB} phase, supporting the hierarchical model in which self-assembly of dimeric molecules with *syn*-parallel orientation formed in the isotropic melt represents the nucleus for its complex helical superstructures in the N_{TB} phase.

INTRODUCTION

The nematic liquid-crystalline phase, the best known for its successful application in flat panel displays, is characterized by such organization in which molecules have no positional order but tend to point to the same direction. This simple molecular arrangement may be swayed by the introduction of chirality, which leads to the cholesteric phase (chiral nematic, N*) or to the blue phase (BP). In 1973 Meyer[1] suggested a theoretical possibility for the existence of a twist-bend nematic (N_{TB}) phase, in which the director of the molecules would precess on a cone forming an oblique helicoidal structure. More recently Dozov[2] and Memmer[3] demonstrated that the formation of the N_{TB} phase does not require molecular chirality, instead it can be facilitated by the shape of bent molecules.

It was only a few years ago, that the unknown nematic phase (N_x) was also experimentally observed, whose unusual characteristic implicated the N_{TB} structure.[4–10] A puzzling combination of smectic textural features but absence of the smectic-like lamellar X-ray diffraction peaks boosted the interest for this new nematic phase. A series of studies[6,9,11–15] focused on investigation of the low-temperature nematic phase formed by 1,7-di-(1"-cyanobiphenyl-4-yl)heptane (CB7CB) reported an evidence for the chiral molecular organization, which is consistent with an oblique helicoidal

structure. These observations include: focal conic, polygonal and rope-like textures displayed by polarizing optical microscopy,[6] helix periodicity observed directly by freeze-fracture transmission electron microscopy (FFTEM),[9,11] flexoelectrically driven electroclinic effect showing extremely short pitch (<10 nm) and ultrafast response times,[12] and discrimination of the prochiral protons in deuterium NMR experiments.[13–15] However, several aspects of the phase are still the subjects of the debate: high viscosity, lack of temperature dependence of the TB helix pitch,[11] presence of various periodicity ranging from 7.7 to 3.4 nm,[9] suppression of induced helicity with the addition of chiral dopants, no electrooptic response in the N_{TB} phase of CB11CB,[16] and locked helical structures of a particular pitch,[17] attribution of the periodic features observed in FFTEM to a thin crystalline layer, easily formed during 'freezing' of the samples,[18]and the possibility for the existence of more than one phase presently identified as the N_{TB}.[19] Several recent studies implied that unconventional properties of the N_{TB} phase originate from self-assembly of the chiral conglomerates.[11,16,17,20] Moreover self-assembly processes were indicated in the uniaxial nematic phase and even in the isotropic state pointing to the hierarchical molecular organization within the N_{TB} phase.[17]

For the majority of the odd-membered dimers displaying two nematic phases, the common structural feature is the methylene link between the spacer and the rigid mesogenic groups.[5,9,20] However, the presence of the N_{TB} phase has also been reported for some odd-membered dimers with an imino linkage[4,8] and for a supermolecular hydrogen-bonded trimer.[21] Due to the limited number of structurally variant compounds exhibiting the low-temperature nematic phase, there is still little known about the structural and electronic aspects influencing its formation.

Herein we report the observation of the N_{TB} phase for some new odd-membered imino-linked cyanobiphenyls that enable a comparative study with methylene and ether linked cyanobiphenyls on impact of the linkage group. In order to unravel the role of structural and electronic factors on the formation of the N_{TB} phase, we have performed a detailed conformational analysis of the methylene,

ether and imino linked cyanobiphenyls, as well as the previously reported less polar *N,N′*-bis[4'-(4''-butyloxybenzoyloxy)benzylidene]-heptane-1,7-diamine **BB_7-4.**[4] Computational analysis of two plausible arrangements, the intercalated and the segregated type, were carried out to provide an information on their relative stabilities. In an attempt to explore a possible organization in the isotropic phase and intermolecular contacts within self-assembly we performed NOESY investigation in the isotropic melt.

RESULTS AND DISCUSSION

Mesomorphic properties.

The molecular structures of new imino-linked cyanobiphenyls and their thermal behavior are shown in Figure 1.

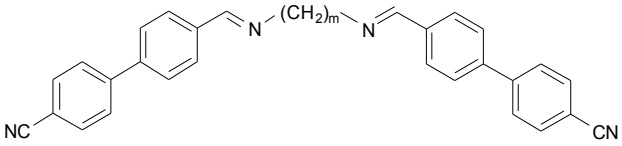

CBI-7-ICB, m=7 Cr 117 [10.54] N_{TB} 123 [0.01] N 149 [0.14] Iso

CBI-9-ICB, m=9 Cr 113 [12.37] N_{TB} 126 [0.03] N 153 [0.36] Iso

Figure 1. Molecular structures and thermal behavior of new imino-linked cyanobipheny dimers. Monotropic transitions are given in parenthesis, transition temperatures in °C, and the dimensionless value of $\Delta S/R$ in brackets. Cr, crystalline phase; N_{TB}, low-temperature nematic phase; N, nematic phase; Iso, isotropic liquid.

The mesomorphic behavior of the dimers **CBI-7-ICB** and **CBI-9-ICB** was determined using polarizing optical microscopy (POM), differential scanning calorimetry (DSC) and X-ray diffraction (XRD). Both dimers display similar mesomorphic properties. Upon heating they show three phase

transitions: melting, followed by the N_{TB}–N transition and isotropization. A nematic phase was identified by the typical marbled texture. The lower temperature mesophase was assigned as N_{TB} phase by direct analogy with the behavior found in **CB7CB**[6], **CB11CB**[16] and benzyloxybenzilidene[4] dimers. In the cooling cycle the N_{TB} phase exhibits a particular textural sequence. The N–N_{TB} transition was accompanied by a change in texture from the marble to a broken fan-like arrangement (Figure 2a). Further cooling resulted in the formation of an elliptical polygonal domain texture from which a characteristic striped structure developed. Contact preparations showed complete miscibility of the N_x phase exhibited by the **BB_7-4**[4] and the low temperature mesophase of **CBI-7-ICB** and **CBI-9-ICB**, confirming that all three imino-linked dimers form the same phase. The results of the XRD measurements on **CBI-7-ICB** and **CBI-9-ICB** in the nematic phases on cooling from the isotropic liquid also closely resemble those for **CB7CB**.[6] Samples aligned in a magnetic field show two kinds of diffuse halos in the wide angle and in the small angle regions, respectively, in both nematic phases. The d values for the maxima of the outer scattering at about 4.4 Å correspond to the lateral distances of the molecules, those of the inner scattering at about 14 Å for **CBI-7-ICB** and at about 15 Å for **CBI-9-ICB** are less than half the molecular lengths. The main effect at the phase transition N – N_{TB} found by XRD is a change of the alignment and a loss of orientation (Figures 2b, c and Figure S1), but also the behavior of the d values for the maxima of the inner scattering with temperature changes at the phase transition as already found for N – N_{TB} transitions.[9] The d values grow with decreasing temperature in the nematic phase, they decrease within the N_{TB} phase from 14.0 (22 °C) to 13.5 Å (116 °C) for **CBI-7-ICB** and from 15.4 (126 °C) to 14.7 Å (116 °C) for **CBI-9-ICB** (Figure 2d, Figure S1 and Table S1).

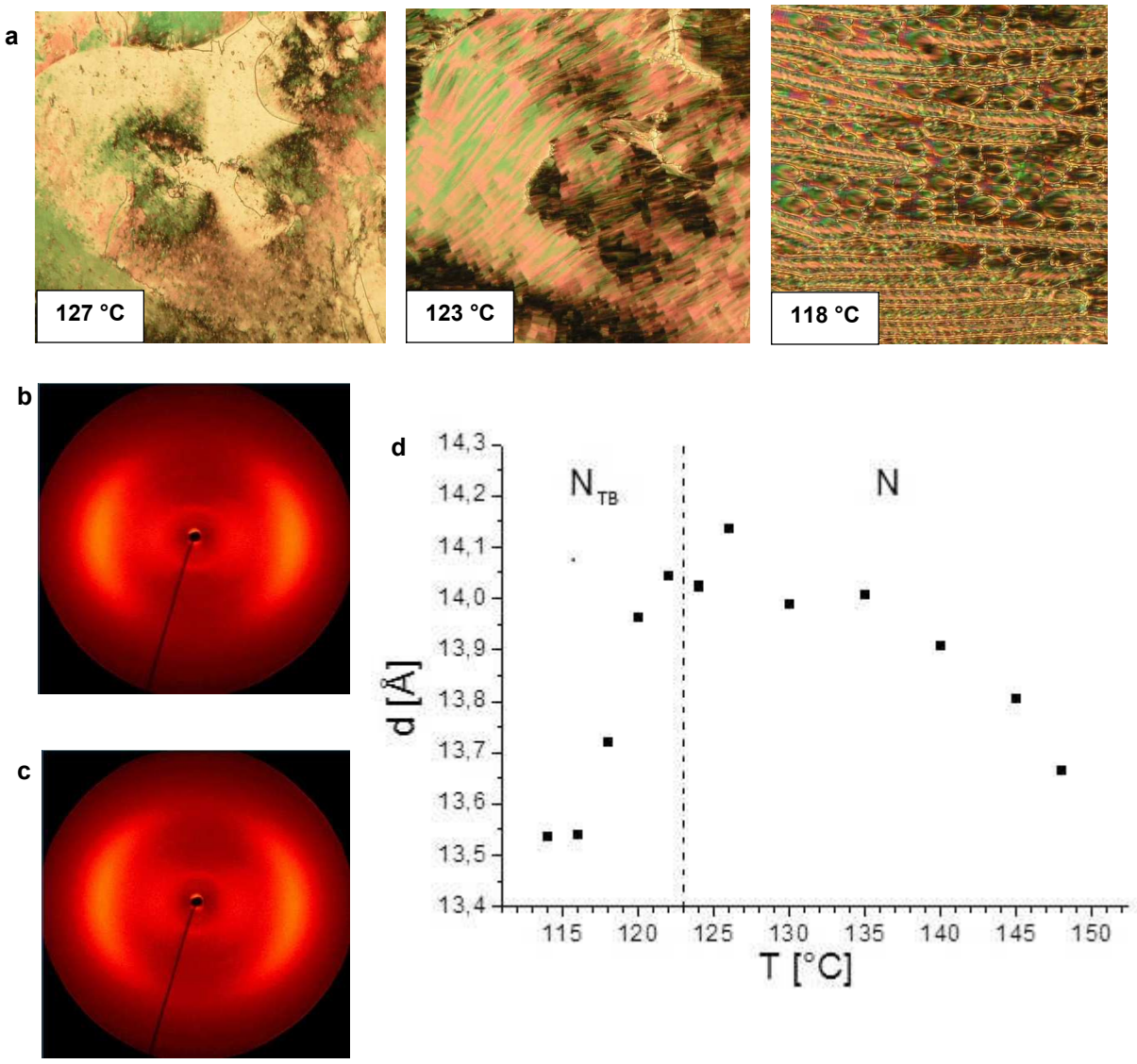

Figure 2. (a) Photomicrographs of the N–N_{TB} transition of **CBI-7-ICB** accompanied by a change in texture from the marble over a broken fan-like to a characteristic striped structure, and XRD patterns of both nematic phases on cooling aligned in the magnetic field: (b) 2D wide angle XRD pattern in the N phase at 135 °C, (c) 2D wide angle XRD pattern in the N_{TB} phase at 118 °C (the comparatively broad diffuse inner scattering on the equator of the patterns originates from the "Bremsberg" radiation of the only Ni-filtered Cu radiation and corresponds to the strong outer diffuse scattering), (d) d value of the intensity maximum of the inner halo depending on the temperature.

It is well known that the transitional properties of liquid-crystalline dimers strongly depend on the molecular shape, which originates from both, the parity of atoms in the spacer and the type of functional group linking the spacer to the mesogenic units.[22] The latter determines an angle between the *para*-axis of the mesogenic unit and the first bond in the spacer, which then results in biaxiality of the molecule.[23] A comparative study of odd-membered methylene (CBmCB) and ether (CBOmOCB) linked cyanobiphenyl dimers demonstrates that the methylene group provides a smaller link angle (113°) than the ether (126°), thus the slightly greater molecular biaxiality of the former. As a result, the clearing entropy is smaller for methylene linked dimers than for those with an ether link.[24,25] Another significant difference between this two kinds of dimers is that the ether-linked dimers form only a single nematic phase,[26] while those with methylene links exhibit also a second liquid-crystalline phase.[6] Recently, this additional mesophase was described as a twist-bend nematic phase and has been attributed to the more pronounced molecular bending.[5–7]

The both newly described imino-linked cyanobiphenyls, **CBI-7-ICB** and **CBI-9-ICB,** display two nematic phases and their thermal properties resemble more those of the methylene-linked derivatives than those with the ether links. For example, the observed entropy changes ($\Delta S/R$) associated with the N-I as well as the N-N_{TB} transitions for **CBI-7-ICB** and **CBI-9-ICB** are comparable in magnitude with the same transitions of dimers having methylene linkage.[5–7] Similar behavior is noticed for benzyloxybenzilidene[4] and salicyl[8] based dimers, both possessing the imino links.

The Molecular Geometry

To evaluate the influence of the linkage group and to gain a better understanding of the forces governing the molecular packing, an extensive computational study with focus on the linkage group

was performed using the Gaussian software package.[27] The input geometries were based on the initial optimization of the mesogen[8] connected with the spacer in the already established all-trans configuration of the carbon atoms.[14]

For the analysis of each dihedral rotation, series of single point constrained geometry optimizations were performed on B3LYP/6-31G level. The rotational barriers were then calculated as energy differences between the two limit geometries. The lowest energy structures were reoptimized using the B3LYP, wB97xD and M06-D3[28] functionals and 6-31G(d,p) basis set with tight convergence criteria.

From the chemistry of biphenyl, its derivatives are known to possess axial chirality, due to the rotation around the bond connecting two phenyl cores. Indeed, the fully optimized structure of **CBI-7-ICB** revealed that the two phenyl cores are mutually rotated by 36° around the biphenyl bond, and that the smallest energy barrier for rotation was ~1.7 kcal mol^{-1}. However, since the biphenyl rotation is also present in ether derivatives for which the N_{TB} phase is not observed, it can safely be excluded as a major factor determining the formation of the phase.

Further, it was suggested that the curvature of the molecule is responsible for the formation of the N_{TB} phase.[23–25] Upon optimization, the variation of the link angle between the linking groups was rather small. Comparing all three cyanobiphenyl derivatives, the methylene and imine derivatives were found slightly more bent than the ether derivative. The analogous C_1-C_2-N_3, C_1-C_2-C_3 and C_1-O_2-C_3 angles were 111°, 112° and 118°, respectively, the latter two being close to the reported ones.[23–25] However, such proximity of the values imply that the curvature of the molecule – although important for the packing model predicted by theory- is not the exclusive structure-property relationship factor determining the formation of the phase.

Another point of interest concerning the optimized structures of the investigated compounds is the rotation between the plane of the mesogen (Π_M) and the plane of the spacer (Π_S) shown

schematically in Figure 3a. This rotation is characterized by the dihedral angle between the planes connecting the *para*-axis of the mesogenic unit (MU) to the methylene or ether linkage group. For the imine, the plane of the mesogen is aligned with the plane of the linkage group due to π-conjugation, so the dihedral rotation of interest is in fact the one around the C-N bond connecting the spacer to the linkage group. The smallest energy barrier for dihedral rotation of one mesogen in **CBI-7-ICB** is 1.9 kcalmol^{-1} at the M06-D3/6-31G(d,p) level. However, the most stable state of the molecule is degenerate due to this rotation, as revealed by any of the functionals used.

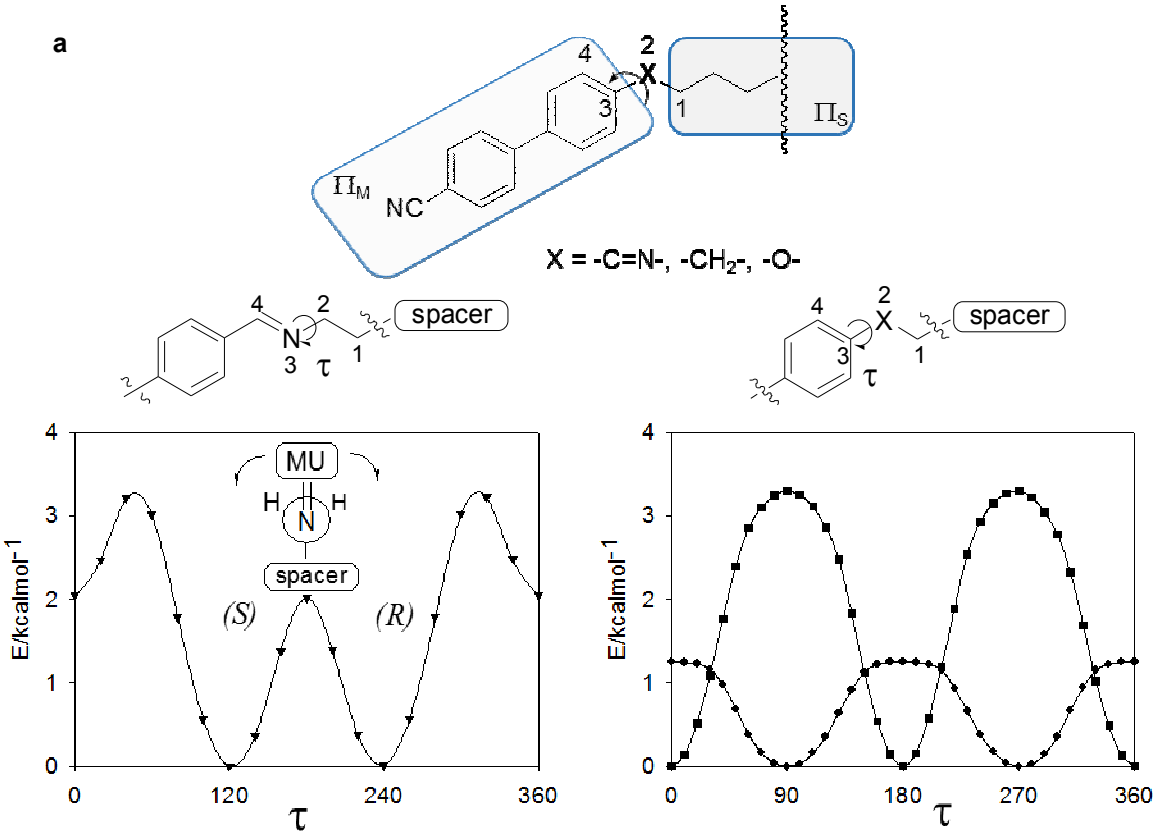

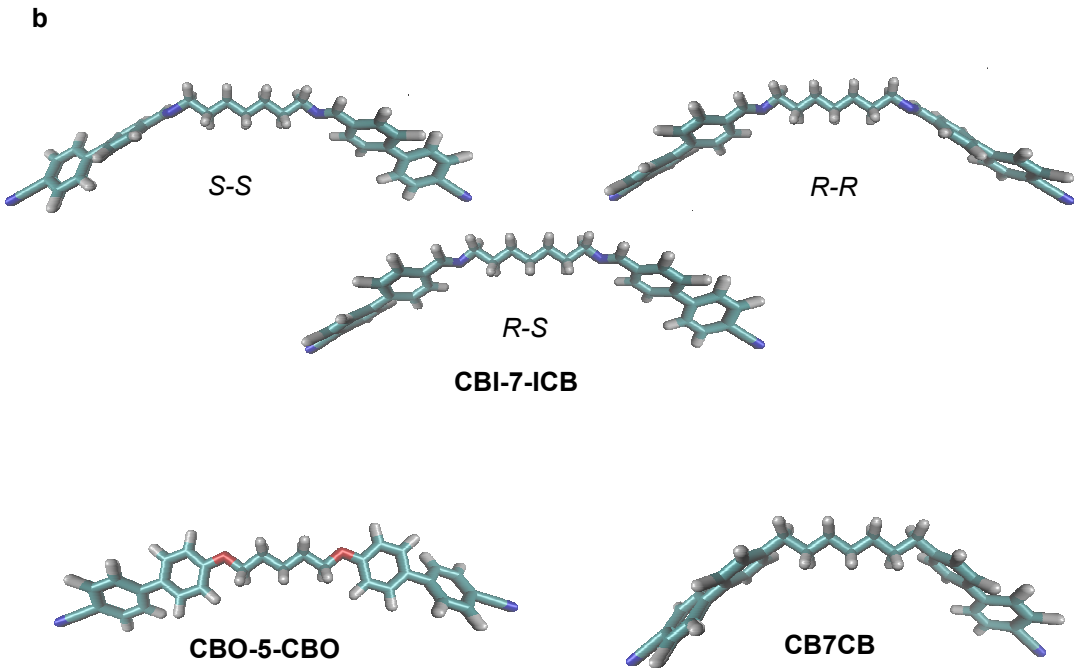

Figure 3. (a) Definition of dihedral rotation (τ) and comparison of imine- (▼), methylene- (●) and ether-linked (■) cyanobiphenyls, (b) most stable conformational states of **CBI-7-ICB, CBO-5-OCB** and **CB7CB**

In the low energy state of the imine derivate, the dihedral angle between Π_M and Π_S may adopt two distinct values, approximately of the same magnitude (~±60°), but opposite sign. In analogy to the nomenclature used for the description of axial chirality, the right handed rotamer may be denoted with (*R*), and the left handed rotamer with (*S*). Since they have equal energy, their distribution in bulk sample should be equal. Thus, for the dimer molecule, two distinct enantiomeric conformers may be identified as *(R)-(R)* and *(S)-(S)*, along with the third, *meso*-conformation *(R)-(S)* (Figure 3b). Analogous dihedral rotation for the **BB_7-4** derivate shows the same behavior, as a general property of the imino linked dimers. This feature of the imino linkage group is due to the asymmetry

of the nitrogen atom possessing a single lone pair, causing the preferential alignment of the plane of the C=N double bond towards one of the two enantiotopic protons of the neighboring -CH_2- in the spacer.

Upon optimization, ether and methylene derivatives show a major difference regarding the angle between the planes Π_M and Π_S. A dihedral angle of $\tau = 0°$ was obtained for the ether derivate, while $\tau = 93°$ was found for the methylene derivate. Consequently, the geometric shape of the former is flat, while that of the latter is spacious (Figure 3b), suggesting a different behavior when packing within the phase. In addition, in the ether a higher energy barrier for dihedral rotation was found (3.50 kcal mol^{-1} compared to 0.89 kcal mol^{-1}) at M06-D3/6-31G(d,p) level. This indicates a more rigid conformation of the ether derivate. For methylene, a partial dihedral rotation may be allowed that would break the symmetry of the molecular conformation and cause the two hydrogens to be in a different chemical surrounding. Solid state NMR study of deuterated **CB7CB** reported that these two enantiotopic hydrogens of the methylene linkage group have lost their equivalence just upon the formation of the N_{TB} phase.[6]

The direction of the dipole momentum in all the studied dimers is perpendicular to the main molecular axis (besides the *meso*-conformation of imine), due to the symmetrical arrangement of the polar mesogen units around the spacer. The methylene derivate is substantially more polar than ether (7.2 Debye compared to 2.3 Debye), since it lacks the polar C-O group producing charge in the direction opposite to the cyano group. Among the imine derivates, **CBI-7-ICB** is more polar than **BB_7-4**, (6.0 and -4.8 Debye respectively). Note also that the dipoles have opposite signs. Both imine derivatives show the N_{TB} phase, as does the salicyl based imino-linked dimer **NS_7-8**[8] whose polarity is rather low (0.1 Debye). Altogether we found no evidence that the magnitude of the dipole moment is responsible for the formation of the phase, as is also noted by Mandle et al.[20,29] On the contrary, it is more likely that the geometry of the molecule is the decisive factor. Until now it was

accepted that molecules forming the N_{TB} phase need to be bent or ″banana-shaped″.[2,3,9] On the basis of our results, a more precise analogy may be ″twisted-banana″ or even ″bent-propeller″, accounting for the large dihedral angle between the plane of mesogen and the plane common to carbon atoms in the spacer. Conformational flipping of the cyanobiphenyl mesogenic core within the flexible dimer has negligible effect on the overall molecular bending (±5°), instead, it contributes to the formation of the chiral conformational states that could lead to helical self-assembled structure. The propeller shape was also associated with the unconventional properties of the biaxial nematic phase (N_b) in the bent-core mesogen[30–35] In bent-core compounds, the central unit defines the bent angle between the two wings of the molecule but the overall shape also depends on the flexibility introduced by the linkage group attaching the wings to the core. The twist of the lateral wings gave rise to the two sets of conformations that may significantly differ in the bend angle as observed for asymmetric BCM[30] but also to enantiochiral molecular states that were held responsible for formation of the twisted states[33] and for the observed spontaneous chiral resolution in the nematic phase.[31,32] Comparative geometrical factors between bent-core mesogen and odd-membered flexible dimers point to a possibility for similar molecular organization in the nematic phases.

Molecular Organization

In addition to the molecular shape, a macroscopic structure is greatly determined by the molecular interactions. It is well known that the strong quadrupolar interactions between the cyanobiphenyl will cause intercalation between the molecules. Hence, the currently proposed model for the N_{TB} phase is based on an *anti*-parallel orientation of the mesogens where the free volume created by quadrupolar interactions is reduced by twisting and formation of a helical structure.[10,12] However the increased number of various dimeric compounds exhibiting the N_{TB} phase implies that it is molecular topology that impels the appearance of the N_{TB} phase, rather than dipolar interactions.[19,20]

Further, the formation of the N_{TB} phase by dimers with? terminal chains longer than the spacer [8,20] suggests a possible existence of another model that will be able to accommodate long terminal chains.

Preliminary DFT calculations for the two types of packing suggest that the *syn*-arrangement is by 22.5 kcal mol^{-1} energetically more favorable than the *anti*-arrangement on M06-D3/6-31G(d,p), although the complete conformational landscape was not explored due to the size of the system (Figure 4). Upon optimization, two molecules in "bent-propeller" conformation are displaced in parallel direction in order to stabilize the π-π interactions. Notably, due to the stabilization, the molecules in the *syn*-parallel packing motif are also slightly rotated with respect to each other.

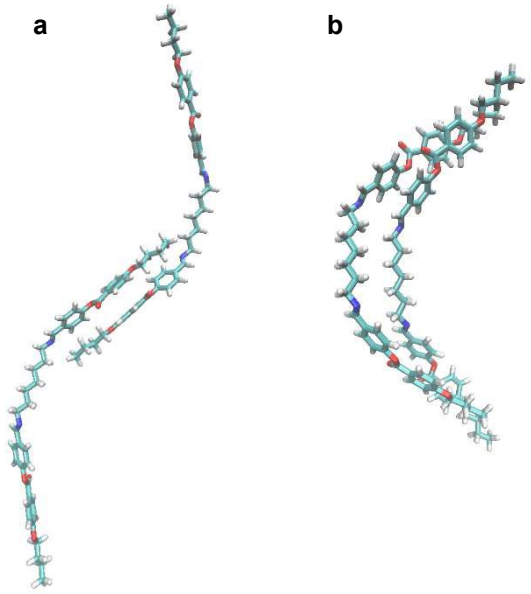

Figure 4. Preliminary structures after optimization on M06-D3/6-31G(d,p): (a) *anti*-parallel arrangement of mesogens, (b) *syn*-parallel arrangement of mesogens.

Recent NMR studies suggest that the organization of the N_{TB} phase involves self-assembly processes in which the molecules are packed in highly correlated chiral domains consisting of molecules with chiral conformations.[17] The very limited variation of the mesogenic order parameter

values between the N and N_{TB} phases implied that the molecular packing in the both phases should be similar although the fast interconversion (on the NMR time scale) between conformations of opposite chirality produces an achiral medium of the N phase. Very low values of the entropy changes for the Iso-N and N-N_{TB} transitions in imino-linked dimers indicate that the local organization might start in the isotropic state. In an attempt to explore the possible organization in the isotropic phase and the intermolecular contacts within self-assembly we performed NOESY investigation in the isotropic melt.

Investigation was carried out on **BB_7-4** because its isotropization temperature (Figure 5a) is lower than those observed for cyanobiphenyls. Also, comparison of ^{1}H NMR spectra of **CBI-7-ICB** and **BB_7-4** recorded in $CDCl_3$ solution (Figure S2) shows that the latter is more suitable for a study of NOE interactions than the cyanobiphenyl series. The signals of aromatic protons in cyanobiphenyls overlap to some extent, while in **BB_7-4** they are conveniently resolved. Moreover, the terminal alkoxy chain may provide more data on the head-to-tail interactions between the molecules than the protonless cyano group. The proton signals of **BB_7-4** in the isotropic melt are significantly broadened in comparison to solution and coupling constants are not visible (Figure 5c). However, they are sufficiently resolved to be assigned as shown in Figure 5c using ^{1}H and ^{1}H-^{1}H COSY spectra (Table S2 and Figure S3). Transition to the nematic phase resulted in the ^{1}H NMR spectra characterized by extensive line broadening over 30 kHz, arising from dipolar couplings, which are no longer averaged to zero by isotropic tumbling. Thus the NOESY spectrum was recorded at 117 °C. All the visible NOE interactions (Figure 5c), and the distance between the protons assigned to these interactions surpass the NOE measurement threshold. For example, the interactions of H15 with H11; H6 with H1 and H2; H7 with H2 and H3 (Figure 5c, d) become clearly visible, all of which are more than 5 Å apart in the individual molecular structure. These can be attributed only to intermolecular interactions between the two neighboring molecules. In control experiment, NOESY

spectra have been taken in DMSO-d_6 solution at 50 °C, in $CDCl_3$ solution at -40 °C (Figure S4) and in the isotropic melt at 135 °C, and the intramolecular interactions between hydrogen atoms only up to 2.5 Å apart were observed. All the visible NOE interactions in point to a *syn*-parallel orientation of the mesogens (Figure 5d) featuring parallel displacement of the molecules to stabilize the π-π interactions.

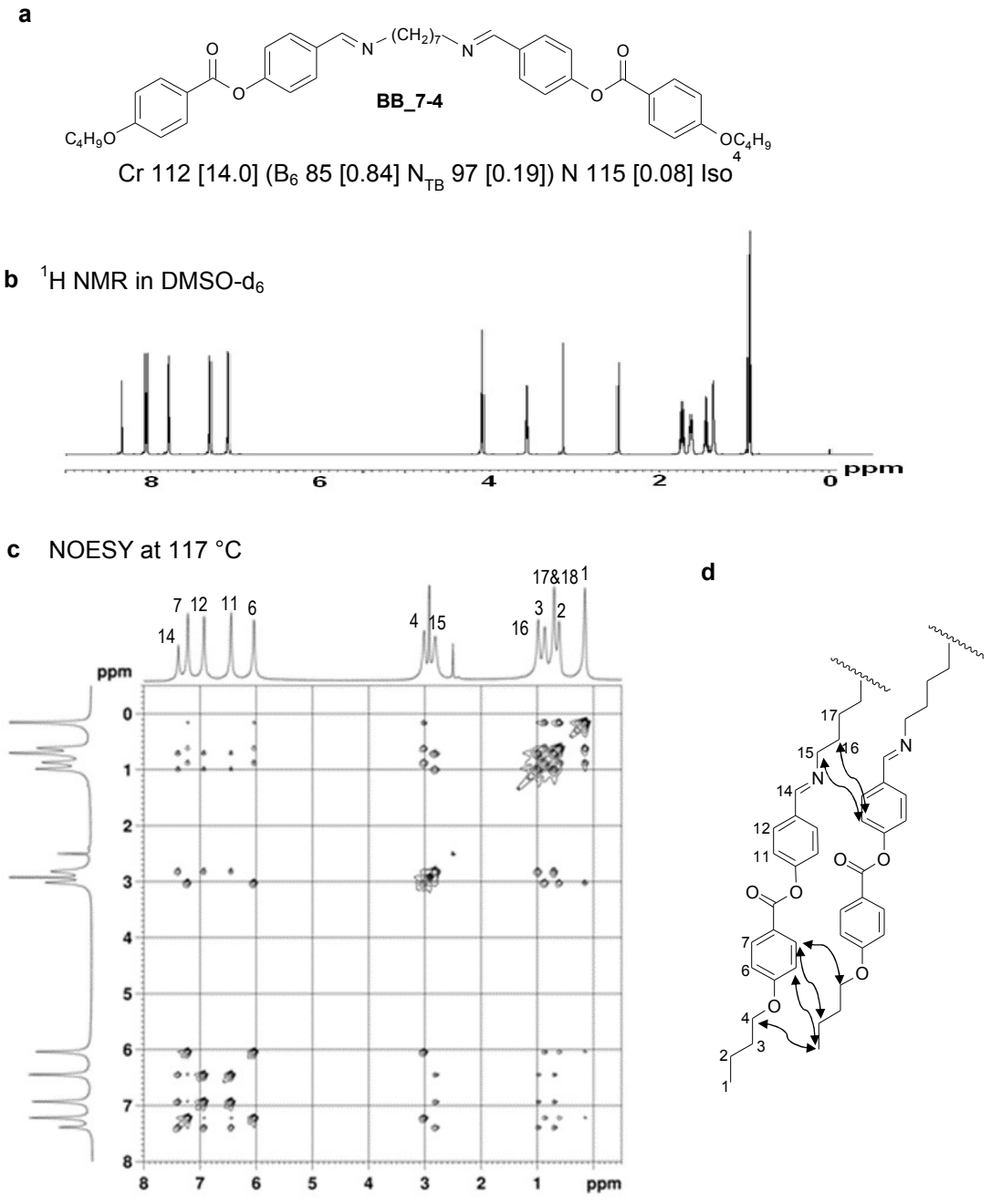

Figure 5. (a) Molecular structure and thermal behavior of **BB_7-4**. Monotropic transitions are given in parenthesis, transition temperatures in °C, and the dimensionless value of $\Delta S/R$ in brackets. (b) ^{1}H NMR spectra of BB_7-4 in DMSO-d_6 solution (c) NOESY spectra of the neat BB_7-4 recorded at 117 °C. (d) Sketch of the most pronounced intermolecular NOESY interactions at 117°C.

This confirms that the formation of the nematic phase is preceded by a self-assembling process that creates small dynamic aggregates having a size of a few molecules. In these aggregates the molecules with *syn*-parallel orientation of the mesogens may also associate/dissociate in some metastable fashion at random positions. Due to the flipping of the mesogenic units the molecules adopt chiral conformational states. Their self-organization following the *syn*-parallel pattern generates nuclei (Figure 6) from which the helical structure might evolve. With decreasing temperature the embryonic aggregates may self-assembly into clusters as implicated by the diffuse X-ray diffraction in the small angle region within the nematic phase[4] and further into highly correlated chiral domains in the N_{TB} phase as suggested by Hoffmann et. al.[17] the exact organization of which is still a controversial issue. These temperature events support the hierarchical model in which organization starts in the isotropic phase, progresses on decreasing the temperature and leads to unconventional properties of the nematic phases. Such organization is not only of fundamental relevance but also opens a possibility to manipulate the nanoscale order what is important for any technological application.

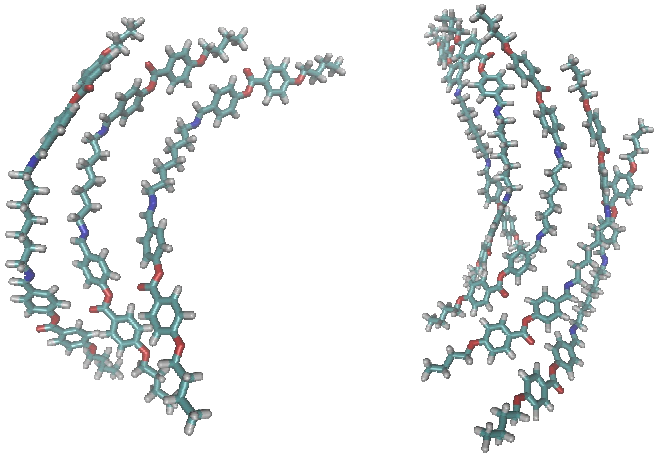

Figure 6. Molecular models for embryonic aggregates consist of 3 to 5 molecules with mutually identical *syn*-parallel orientation of all mesogens.

EXPERIMENTAL SECTION

General Information.

All the solvents were either *puriss p.a.* quality or distilled over appropriate drying reagents. All the other reagents were used as purchased from Aldrich. NMR spectra were recorded on Bruker AV-600 instrument in DMSO-d_6 with $SiMe_4$ as internal standard unless stated otherwise. Phase transition temperatures and textures were determined using an Olympus BX51 polarizing microscope equipped with a Linkam TH600 hot stage and PR600 temperature controller. Enthalpies of transition were determined from thermograms recorded on Perkin-Elmer Diamond DSC, operated at scanning rates of 5 °C min^{-1}. To perform X-ray diffraction measurements samples of **CBI-7-ICB** and **CBI-9-ICB** were kept in glass capillaries (∅ 1 mm) in a temperature controlled heating stage and partially aligned in a magnetic field on cooling (1 K/min) from the isotropic liquid. 2D patterns were recorded by an area detector VÅNTEC500 (Bruker AXS) using Ni-filtered CuKα radiation. The one- and two dimensional homo- and heteronuclear ^{1}H and ^{13}C NMR spectra were recorded

with a Bruker AV-600 spectrometer, operating at 600.133 MHz for the ^{1}H nucleus and 150.917 MHz for the ^{13}C nucleus. The following measurement techniques were used: standard ^{1}H, ^{13}C gated proton decoupling, APT, COSY, NOESY, HMQC and HMBC. To record the NMR spectra of the neat sample the glass capillary (∅ 1 mm) filled with solid compound was immersed into standard 5 mm NMR tube filled with DMSO-d_6. The temperature is regulated by a Bruker B-VT 3000 temperature unit. The actual temperature was verified with ethylene glycol before and after the experiment. Chemical shifts are reported in ppm, downfield of tetramethylsilane. FID resolution in ^{1}H NMR and ^{13}C NMR spectra was 0.29 Hz and 0.54 Hz per point, respectively. The NOESY spectra were measured in phase-sensitive mode, with mixing time of 0.50 s and 16 or 64 scans per each increment. The spectral width was 6127.45 Hz, 2048 points in F2 dimension and 512 increments in F1 dimension, subsequently zero-filled to 1024 points. The resulting FID resolution was 2.99 Hz/point and 11.96 Hz/point in F2 and F1 dimensions, respectively.

Synthesis.

The novel imino-linked cyanobiphenyl dimers **CBI-7-ICB** and **CBI-9-ICB** were prepared from 4-bromo-benzonitrile and 4-formylphenylboronic acid employing Suzuki coupling[36] followed by condensation with appropriate α,ω-diamino alkane (Scheme 1). N,N'-bis[4'-(4''-butyloxybenzoyloxy)benzylidene]-heptane-1,7-diamine (**BB_7-4**) was prepared as described previously and its physical properties are consistent with the published data.[4]

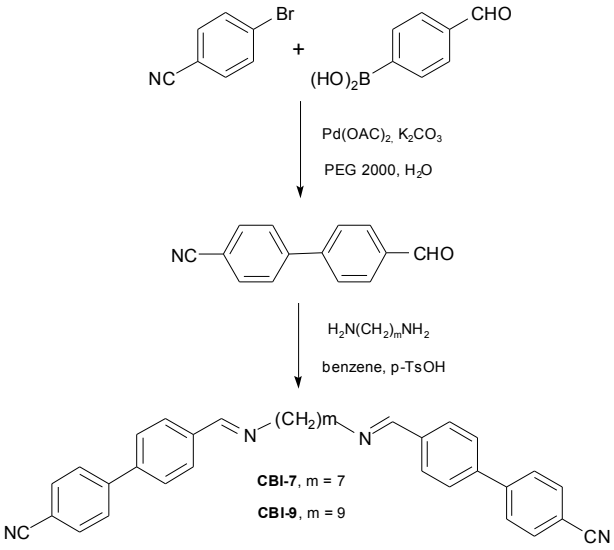

Scheme 1. Synthesis of imino-linked cyanobiphenyl dimers **CBI-7-ICB** and **CBI-9-ICB**.

4-Formyl-biphenyl-4'-carbonitrile[36] A mixture of Na_2CO_3 (1.06 g, 10 mmol), $Pd(OAc)_2$ (56 mg, 5 mol %), PEG 2000 (17.5 g) and water (15 mL) was heated to 50 °C under inert atmosphere with stirring. Afterwards, 4-bromo-benzonitrile (0.91 g, 5 mmol) and 4-formylphenylboronic acid (1.12 g, 7.5 mmol) were added to the solution, and the reaction was carried out at 50 °C under inert atmosphere. After 45 min. the reaction mixture was cooled to room temperature, diluted with water (100 mL), and extracted with diethyl ether (3 x 50 mL). The combined organic extracts were washed with brine (50 mL), dried over anhydrous Na_2SO_4 and concentrated in vacuum. The crude product was purified by column chromatography on silica gel using CH_2Cl_2 as eluent affording product (0.88 g, 85 %) as white solid. mp. 59-160 °C; ^{1}H-NMR ($CDCl_3$) δ/ppm: 7.72-7.80 (m, 6H), 8.00 (d, J=8.4 Hz, 2H), 10.09 (s, 1H); ^{13}C-NMR ($CDCl_3$) δ/ppm: 112.2, 118.5, 127.9, 128.0, 130.4, 132.8, 136.1, 144.1, 144.9, 191.6.

General procedure for the preparation of imines. A solution of the appropriate α,ω-diamine (1 mmol) in benzene (2 mL) was added dropwise to a hot solution of 4-formyl-biphenyl-4'-carbonitrile

(2 mmol) in benzene (25 mL) and catalytic amount of *p*-toluenesulfonic acid. The reaction mixture was heated under reflux for 1 h under argon and then 15 mL of benzene was distilled off. The hot residue was filtered and mixed with n-hexane (25 mL). The pure crystalline product, which precipitated on cooling, was separated by filtration.

N,N'-bis(4,4'-cyanobiphenymethylidene)-heptane-1,7-diamine, **CBI-7-ICB.** Yield, 60 %; PT (°C): Cr 117 N_{TB} 123 N 149 Iso; ^{1}H-NMR ($CDCl_3$) δ/ppm: 1.41-1.47 (m, 6 H), 1.71-1.81 (m, 4H), 3.67 (t, J = 6.8 Hz, 4H), 7.65 (d, J = 8.4 Hz, 4H Ar), 7.71-7.78 (m, 8H Ar), 7.86 (d, J = 8.4 Hz, 4H Ar), 8.34 (s, 2H); ^{13}C-NMR ($CDCl_3$) δ/ppm: 27.3, 29.2, 30.9, 61.9,111.4, 118.8, 127.4, 127.7, 128.7, 132.6, 136.6, 141.0, 144.9, 159.9. Found: C, 82.50; H, 6.25; N, 11.13. Calc for $C_{35}H_{32}N_4$: C, 82.64; H, 6.34; N, 11.01.

N,N'-bis(4,4'-cyanobiphenymethylidene)-nonane-1,9-diamine, **CBI-9-ICB.** Yield, 82 %; PT (°C): Cr 113 N_{TB} 126 N 153 Iso; ^{1}H-NMR ($CDCl_3$) δ/ppm: 1.37-1.43 (m, 10 H), 1.69-1.79 (m, 4H), 3.66 (t, J = 6.8 Hz, 4H), 7.66 (d, J = 8.3 Hz, 4H Ar), 7.71-7.78 (m, 8H Ar), 7.86 (d, J = 8.3 Hz, 4H Ar), 8.34 (s, 2H); ^{13}C-NMR ($CDCl_3$) δ/ppm: 27.3, 29.4, 29.5, 30.9, 61.9, 111.3, 118.8, 127.4, 127.7, 132.6, 136.6, 140.9, 144.9, 159.8. Found: C, 82.68; H, 6.73; N, 10.57. Calc for $C_{37}H_{36}N_4$: C, 82.80; H, 6.76; N, 10.44.

CONCLUSION

Here we have reported on the synthesis and thermal properties of new cyanobiphenyl dimers with an imino linkage group exhibiting the N_{TB} phase. A comparative computational study of the methylene, ether and imino linked cyanobiphenyls, as well as some less polar imino linked dimers showed that the geometry of the molecule is the predominating factor in the formation of the N_{TB} phase. In addition to the already known requirement for the curvature of the molecule, the twist caused by the

dihedral angles between the plane of the spacer and the planes of the mesogens was identified as an important structural difference between the compounds with and without the N_{TB} phase. Computational analysis of possible types of molecular packing suggests that the *syn*-parallel arrangement of the dimeric molecules is energetically more favorable than the *anti*-parallel. The NOESY experiments showed that the formation of the nematic phase is preceded by a self-assembling process that creates embryonic dynamic aggregates and the NOE interactions pointed to a *syn*-parallel orientation of the mesogens featuring parallel displacement of the molecules. Overall, combination of experimental, computational and NMR studies support the model of a hierarchical organization for the controversially discussed N_{TB} phase that involves self-assembly of dimeric molecules with *syn*-parallel orientation as the basis for its complex helical superstructures

Electronic Supplementary Information (ESI) available:

ACKNOWLEDGEMENTS

The authors thank the Croatian Science Foundation (grant number, IP-2014-09-1525) and the Ministry of Science, Education and Sports of the Republic of Croatia for financial support (grant number, 098-0982929-2917). We are also grateful to Dr. Nađa Došlić (Theoretical Chemistry Group, Ruđer Bošković Institute, Zagreb) for helpful discussions and suggestions concerning the electronic structure calculations

REFERENCES

1 R. Balian and G. Weill, *Molecular Fluids Les Houches Lectures 1973*, Routledge, London u.a., 1976.

2 I. Dozov, *EPL Europhys. Lett.*, 2001, 56, 247–253.

3 R. Memmer, *Liq. Cryst.*, 2002, 29, 483–496.

4 M. Šepelj, A. Lesac, U. Baumeister, S. Diele, H. L. Nguyen and D. W. Bruce, *J. Mater. Chem.*, 2007, 17, 1154–1165.

5 V. P. Panov, M. Nagaraj, J. K. Vij, Y. P. Panarin, A. Kohlmeier, M. G. Tamba, R. A. Lewis and G. H. Mehl, *Phys. Rev. Lett.*, 2010, 105, 167801.

6 M. Cestari, S. Diez-Berart, D. A. Dunmur, A. Ferrarini, M. R. de la Fuente, D. J. B. Jackson, D. O. Lopez, G. R. Luckhurst, M. A. Perez-Jubindo, R. M. Richardson, J. Salud, B. A. Timimi and H. Zimmermann, *Phys. Rev. E*, 2011, 84, 031704.

7 P. A. Henderson and C. T. Imrie, *Liq. Cryst.*, 2011, 38, 1407–1414.

8 M. Šepelj, U. Baumeister, T. Ivšić and A. Lesac, *J. Phys. Chem. B*, 2013, 117, 8918–8929.

9 V. Borshch, Y.-K. Kim, J. Xiang, M. Gao, A. Jákli, V. P. Panov, J. K. Vij, C. T. Imrie, M.-G. Tamba and G. H. Mehl, *Nat. Commun.*, 2013, 4, 2635.

10 D. Chen, M. Nakata, R. Shao, M. R. Tuchband, M. Shuai, U. Baumeister, W. Weissflog, D. M. Walba, M. A. Glaser and J. E. Maclennan, *Phys. Rev. E*, 2014, 89, 022506.

11 D. Chen, J. H. Porada, J. B. Hooper, A. Klittnick, Y. Shen, M. R. Tuchband, E. Korblova, D. Bedrov, D. M. Walba and M. A. Glaser, *Proc. Natl. Acad. Sci.*, 2013, 110, 15931–15936.

12 C. Meyer, G. R. Luckhurst and I. Dozov, *Phys. Rev. Lett.*, 2013, 111, 067801.

13 L. Beguin, J. W. Emsley, M. Lelli, A. Lesage, G. R. Luckhurst, B. A. Timimi and H. Zimmermann, *J. Phys. Chem. B*, 2012, 116, 7940–7951.

14 J. W. Emsley, M. Lelli, A. Lesage and G. R. Luckhurst, *J. Phys. Chem. B*, 2013, 117, 6547–6557.

15 C. Greco, G. R. Luckhurst and A. Ferrarini, *Phys. Chem. Chem. Phys.*, 2013, 15, 14961–14965.

16 R. J. Mandle, E. J. Davis, C. T. Archbold, S. J. Cowling and J. W. Goodby, *J. Mater. Chem. C*, 2014, 2, 556–566.

17 A. Hoffmann, A. G. Vanakaras, A. Kohlmeier, G. H. Mehl and D. J. Photinos, *Soft Matter*, 2014, 11, 850–855.

18 E. Gorecka, M. Salamonczyk, A. Zep, D. Pociecha, C. Welch, Z. Ahmed and G. H. Mehl, *Liq. Cryst.*, 2015, 42, 1–7.

19 R. J. Mandle, E. J. Davis, C.-C. A. Voll, C. T. Archbold, J. W. Goodby and S. J. Cowling, *Liq. Cryst.*, 2015, 42, 688–703.

20 R. J. Mandle, E. J. Davis, C. T. Archbold, C. C. A. Voll, J. L. Andrews, S. J. Cowling and J. W. Goodby, *Chem. - Eur. J.*, 2015, 21, 8158–8167.

21 S. M. Jansze, A. Martínez-Felipe, J. M. D. Storey, A. T. M. Marcelis and C. T. Imrie, *Angew. Chem. Int. Ed.*, 2015, 54, 643–646.

22 C. T. Imrie and P. A. Henderson, *Chem. Soc. Rev.*, 2007, 36, 2096–2124.

23 A. Ferrarini, G. R. Luckhurst, P. L. Nordio and S. J. Roskilly, *Liq. Cryst.*, 1996, 21, 373–382.

24 P. J. Barnes, A. G. Douglass, S. K. Heeks and G. R. Luckhurst, *Liq. Cryst.*, 1993, 13, 603–613.

25 P. A. Henderson, J. M. Seddon and C. T. Imrie, *Liq. Cryst.*, 2005, 32, 1499–1513.

26 J. W. Emsley, G. R. Luckhurst, G. N. Shilstone and I. Sage, *Mol. Cryst. Liq. Cryst.*, 1984, 102, 223–233.

27 M. J. Frisch, G. W. Trucks, H. B. Schlegel, G. E. Scuseria, M. A. Robb, J. R. Cheeseman, J. A. Montgomery, Jr., T. Vreven, K. N. Kudin, J. C. Burant, J. M. Millam, S. S. Iyengar, J. Tomasi, V. Barone, B. Mennucci, M. Cossi, G. Scalmani, N. Rega, G. A. Petersson, H. Nakatsuji, M. Hada, M. Ehara, K. Toyota, R. Fukuda, J. Hasegawa, M. Ishida, T. Nakajima, Y. Honda, O. Kitao, H. Nakai, M. Klene, X. Li, J. E. Knox, H. P. Hratchian, J. B. Cross, V. Bakken, C. Adamo, J. Jaramillo, R. Gomperts, R. E. Stratmann, O. Yazyev, A. J. Austin, R. Cammi, C. Pomelli, J. W.

Ochterski, P. Y. Ayala, K. Morokuma, G. A. Voth, P. Salvador, J. J. Dannenberg, V. G. Zakrzewski, S. Dapprich, A. D. Daniels, M. C. Strain, O. Farkas, D. K. Malick, A. D. Rabuck, K. Raghavachari, J. B. Foresman, J. V. Ortiz, Q. Cui, A. G. Baboul, S. Clifford, J. Cioslowski, B. B. Stefanov, G. Liu, A. Liashenko, P. Piskorz, I. Komaromi, R. L. Martin, D. J. Fox, T. Keith, M. A. Al-Laham, C. Y. Peng, A. Nanayakkara, M. Challacombe, P. M. W. Gill, B. Johnson, W. Chen, M. W. Wong, C. Gonzalez and J. A. Pople, *Gaussian 09, Revision A.02*, 2009.

28 S. Grimme, J. Antony, S. Ehrlich and H. Krieg, *J. Chem. Phys.*, 2010, 132, 154104.

29 R. J. Mandle, E. J. Davis, S. A. Lobato, C.-C. A. Vol, S. J. Cowling and J. W. Goodby, *Phys. Chem. Chem. Phys.*, 2014, 16, 6907–6915.

30 R. Y. Dong and A. Marini, *J. Phys. Chem. B*, 2009, 113, 14062–14072.

31 V. Görtz, C. Southern, N. W. Roberts, H. F. Gleeson and J. W. Goodby, *Soft Matter*, 2009, 5, 463–471.

32 V. Görtz, *Liq. Cryst. Today*, 2010, 19, 37–48.

33 S. D. Peroukidis, A. G. Vanakaras and D. J. Photinos, *Phys. Rev. E*, 2011, 84, 010702.

34 C. Greco, G. R. Luckhurst and A. Ferrarini, *Soft Matter*, 2014, 10, 9318–9323.

35 C. Greco, A. Marini, E. Frezza and A. Ferrarini, *ChemPhysChem*, 2014, 15, 1336–1344.

36 L. Liu, Y. Zhang and Y. Wang, *J. Org. Chem.*, 2005, 70, 6122–6125.